Student Journal of Energy Research

Volume 2 | Number 1 Article 2

2017

Ray Tracing Technique for the Optimal Design of an Air Heater Concentrating Collector

Fernando Guerreiro
Dublin Institute of Technology, fernando.guerreiro@mydit.ie

Recommended Citation

Guerreiro, Fernando (2017) "Ray Tracing Technique for the Optimal Design of an Air Heater Concentrating Collector," *Student Journal of Energy Research*: Vol. 2: No. 1, Article 2.
doi:10.21427/D71S73
Available at: https://arrow.tudublin.ie/sjer/vol2/iss1/2

Ray Tracing Technique for the Optimal Design of an Air Heater Concentrating Collector

Fernando S. Guerreiro*
*Dublin Institute of Technology (DIT), Dublin, Ireland

Corresponding Author: Fernando S. Guerreiro, email: fernando.guerreiro@mydit.ie

ABSTRACT: There is a wide range of micro and macro renewable and sustainable energy methods available for reducing the inefficient use of fossil fuels, minimising carbon emissions and maximising energy use in a clean and environment-friendly process. Solar energy plays an important role due to its abundance and ubiquity. Solar air heaters convert solar energy into hot air to be used for heating and drying of various products. The objective of this paper is to define and optimise the geometry of an inverted absorber compound parabolic concentrating (IACPC) collector for air heating. This optimisation was developed based on an optical analysis performed by means of a ray tracing technique. The optimal geometry was designed to absorb the highest amount of thermal energy with the minimum quantity of reflective material and to operate for at least 8 hours a day during summer. Based on the energy output of the optical concentrator developed, the system has the potential to reduce energy demands for buildings, living accommodation and drying materials.

KEYWORDS: Ray Tracing, Air Heater, Inverted Absorber, Asymmetric Parabolic Concentrator, Optical Efficiency

1 Introduction

Currently there is a need to explore renewable energy sources in order to minimise carbon emissions from fossil fuels and maximise the use of a clean and environment-friendly process. Solar energy is one of the most abundant types of renewable sources and its conversion into thermal energy is easy and widely accepted. Moreover, solar energy plays an important role for air heating systems as the air is usually the final receiver of the thermal energy (Tyagi et al., 2012). Solar air heaters are devices that convert solar thermal energy into hot air to be used for many applications: space heating of buildings and dwellings, timber seasoning, and drying of agricultural products (Alta et al., 2010).

Concentrators offer a reasonable alternative to flat-plate collectors for delivering hot air flows at higher temperatures (Duffie & Beckman, 2013). They are designed to receive solar radiation through an aperture area and direct it towards a smaller absorber area by employing a reflective material (Goswami, 2015). Theoretical and experimental analyses have been undertaken in relation to asymmetric inverted absorber compound parabolic concentrating (IACPC) collectors with the aim of supressing heat losses by placing the absorber horizontally and facing towards the ground (Rabl, 1976). Kothdiwala et al. (1996) and Eames et al. (1996) performed optical and thermal analyses on this type of collector in order to evaluate the effect of the cavity height beneath the absorber. Kothdiwala et al. (1997) undertook experimental investigation on this collector for water heating at different cavity heights. Kothdiwala et al. (1999) compared the thermal efficiency of an IACPC to that of a tubular absorber CPC.

An IACPC was designed to be used as a solar air heater collector by Shams (2013). This collector had a perforated absorber surface made of carbon fibre placed at a fixed cavity height. This air heater concentrating collector is glazed, has a concentration ratio of 2.0, and it was optically characterised and experimentally tested at different air flow rates.

The design and analysis of solar concentrators are mostly based on ray tracing (Welford & Winston, 1989). Ray tracing is the technique that traces the path of the light represented by multiple straight-line elements. The technique can include the effects of reflection, refraction, or shading. This tool can provide relevant information regarding the collector's performance, such as:

- average number of reflections before the incoming rays reach the absorber plate;
- beam optical efficiency as a function of the incidence angle;
- diagram of the ray's path and reflection points (Mallick et al., 2007);
- intensity of energy distributed along the absorber surface (Shams, 2013);
- characterisation of the system's optical behaviour for heat transfer modelling and simulation;
- verification of rejected incoming rays for a particular reflector geometric shape (Wu, 2009);
- comparison of the optical performance between two different systems (Zacharopoulos et al.,2000).

Hence, the objective of this paper is to define the optimal geometry of an air heater IACPC collector with a perforated absorber based on optical analysis, with the assistance of a ray tracing technique. Considering eight hours of solar radiation per day in the summer, the optimal geometry must absorb the highest amount of solar thermal energy. The collector will be used for air heating purposes.

2 Methodology

2.1 Collector's specifications

The proposed collector is a combination of an inverted

Figure 1: Isometric view of the IACPC collector to be designed.

perforated (transpired) absorber and asymmetric compound parabolic concentrator (ACPC), as shown in Figure 1 and Figure 2.

The device can be divided to the three sections outlined below.

- Primary section: this consists of two asymmetric parabolic reflectors that reflect solar rays coming through the aperture and concentrates them to the secondary section.
- Secondary section: this comprises of a circular reflector, responsible for reflecting all the incoming rays upwards towards the tertiary section.

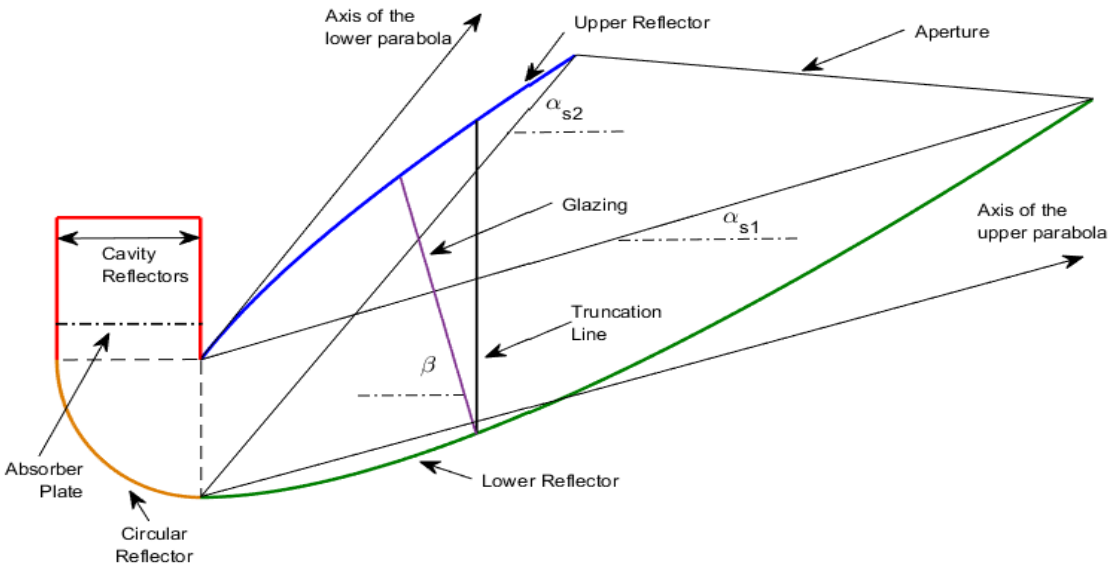

Figure 2: Solar collector's cross section sketch.

- Tertiary section: this consists of a cavity composed of two vertical straight reflectors that receive some of the solar rays from the secondary section and directs them towards the absorber surface. This section has the function of keeping the convection supressed at the absorber through the formation of

a hot air pocket within the cavity (Eames et al., 1996).

The absorber surface is inverted to reduce radiation loss and stabilise the thermal layers below which improves the heat transfer mechanism. Additionally, it is perforated to allow the airflow to percolate through the holes, thus enhancing the heat transfer from the absorber to the flow (Shams et al., 2016).

The aperture at the vertical position (at the truncation line indicated in Figure 2) has been set to a width of 330 mm (W_{apt}) to allow three collectors per meter height to be hung on the wall, thus avoiding over-shading. The glazing placed in the primary section works as a heat trap. During outdoor operation, the glazing offers protecting for the interior of the unit against the weather. Its position at a given inclination β seeks to maximise light transmittance during the operation period.

Considerations have also been given to the angles of the axes of both parabolas (α_{s1} and α_{s2}), which influence the primary section shape. The selection of such variables must take into account the compromise between optical efficiency and concentration ratio (ratio of aperture area to absorber area) to collect more solar radiation.

Besides the variables previously mentioned, there is a minimum requirement for the collector's full operation: 8 hours a day over the summer (93 days) in Dublin (53º latitude), from 8am to 4pm. This means that all incoming direct solar rays must go towards the absorber during that period, accepting solar radiation from 17º to 60º of altitude angles.

2.2 Optical Modelling

To assist the optical analysis, a 2D ray tracing algorithm was implemented in Matlab® and used to trace the solar rays that come through the aperture and strike the reflectors before reaching the absorber surface. Figure 3 illustrates the ray tracing diagram plotted by this algorithm.

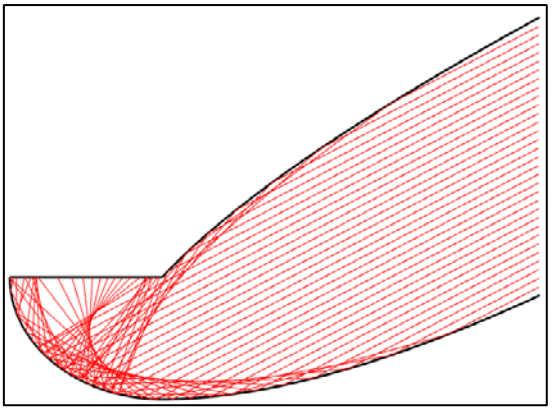

Figure 3: Ray tracing diagram. 31 rays were used for illustrative purpose.

The following assumptions were used for the algorithm development:

- all reflectors are specular, i.e., the incident angle is equal to the reflected angle in relation to the normal at the intersection point;
- the reflector reflectance (ρ) is 0.95 (95% of the ray's energy is reflected at each reflection);
- 3,300 equally spaced solar rays were used, each one carrying equal amounts of energy (E) regardless of their solar altitude;
- the absorber absorptance (α_{abs}) is 0.85; and
- a 4-mm thick low iron glass was employed with a refraction index of 1.526 and an extinction coefficient of 4 m^{-1}. The glazing transmittance (τ_g) was calculated by using equations described in Duffie and Beckman (2013).

It is important to define the beam optical efficiency, which is the ratio between the absorbed energy and the incoming energy. Equation (1) represents the formula used to calculate this efficiency as a function of the solar altitude angle α_p and the incident angle θ:

$$\eta_B = \frac{\sum_{i=1}^{3000} \rho^{n_i} \tau_g(\theta) \alpha_{abs} E_i}{\sum_{i=1}^{3000} E_i} \quad (1)$$

where n_i is the number of reflections of the solar ray i. The incident angle is the angle between the solar altitude and the normal line to the glazing surface and can be calculated from Equation (2).

$$\theta = \alpha_p - (90 - \beta) \quad (2)$$

Considering the full operational requirements in summer, Equation (3) defines the mean optical

efficiency within the solar altitude angle range (17º – 60º):

$$\eta_{MO} = \frac{\sum_{j=17^o}^{60^o}\sum_{i=1}^{3000} \rho^{n_i}\tau_g(\theta)\alpha_{abs}E_i}{\sum_{j=17^o}^{60^o}\sum_{i=1}^{3000} E_i} \quad (3)$$

It is important to define the global optical efficiency η_{GO} that corresponds to the fraction of incident solar energy measured at the site throughout the period analysed – 8 hours a day (28,800 seconds) for 93 days – the calculation of which is presented by Equation (4) (Goswami, 2015):

$$\eta_{GO} = \frac{\sum_{m=1}^{93}\sum_{k=1}^{28800} \rho^{n}\tau_g\alpha_{abs}\left[G_{B,mk}\cos\theta_{mk} + \frac{G_{D,mk}}{C}\right]}{\sum_{m=1}^{93}\sum_{k=1}^{28800}\left[G_{B,mk} + G_{D,mk}\right]} \quad (4)$$

where G_B is the beam or direct radiation, G_D is the diffuse radiation, and C is the concentration ratio. The diffuse radiation distribution was assumed to be isotropic, which implies that the diffuse component entering the collector is directly proportional to 1/C (Rabl, 1976). The data of G_B and G_D are from 2014 and 2015 in Dublin.

Lastly, the total absorbed energy S_T can be calculated by Equation (5), which is the portion of the incident energy on the aperture expressed in units of MJ per m^2 of absorber.

$$S_T = G_T\eta_{GO}C \quad (5)$$

where G_T is the total solar radiation from those periods. This optical analysis did not include the tertiary section because the position of the absorber surface in the cavity must be selected based on experimental results or fluid dynamic analysis, which is beyond the scope of this study. For the collector's design, the reflector's height of the tertiary section will have the value of the absorber width.

3 Results and Discussion

To achieve the optimum design, the analysis started from the collector with the following characteristics: α_{s1} = 17º, α_{s2} = 60º, collector length of 1,250 mm and β = 90º (vertical position). From this, variations in β and α_{s2} were investigated to establish the final design. Using SolidWorks®, the sketch of the initial design was performed (Figure 4) and from this, the absorber width was found with the aim of achieving the maximum concentration ratio. Hence, the absorber width (W_{abs}) is 145 mm with a concentration ratio (C) of 2.276.

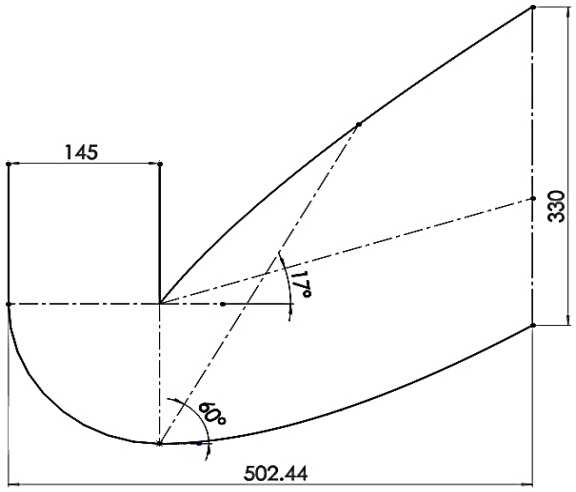

Figure 4: Collector's initial design (mm).

Once the concentration ratio of the collector is set, the next step was to run the ray tracing algorithm to find the optimal glazing inclination that maximises S_T. At this inclination energy losses through the glass are minimized. Figure 5 shows the variation of S_T and η_{MO} as function of β.

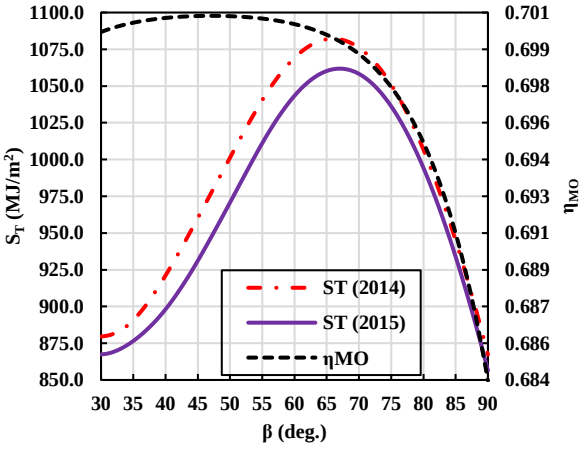

Figure 5: Total absorbed energy and mean optical efficiency *versus* glazing inclination.

From this result, the optimum inclination is approximately 66º, leading to η_{MO} of 0.6998 and S_T of 1,082 MJ/m^2 for 2014 solar data for Dublin and 1,062 MJ/m^2 for 2015 data. Compared to the initial design (β = 90º), S_T for the average of 2014 and 2015

was increased by almost 25% and η_{MO} by approximately 2.3%. It was also observed that the inclinations that result in the highest values of mean optical efficiency (with a maximum of 0.7008) are close to 53º. However, the position at these inclinations does not provide the highest amount of total absorbed energy, as the energy at 66º of glazing inclination is almost 12% higher than that at the position of maximum η_{MO}.

The next analysis evaluates the influence of the angle of the lower parabola axis α_{s2}. Figure 6 shows the variation of S_T and η_{MO} as a function of α_{s2}.

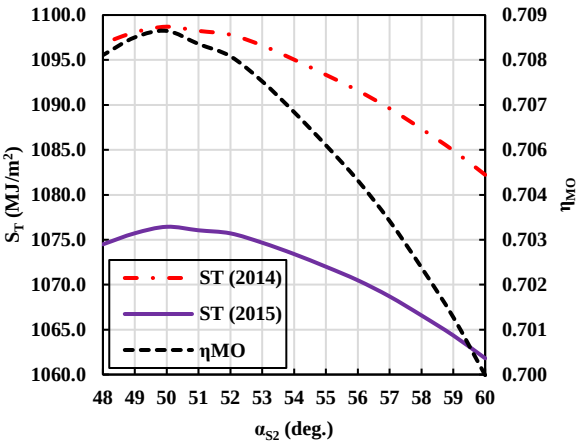

Figure 6: Total absorbed energy and mean optical efficiency *versus* angle of the lower parabola axis. Glazing inclination of 66º.

It is noted that the influence of α_{s2} on S_T and η_{MO} is less significant than that of β on the same dependent variables. The highest values were achieved at α_{s2} = 50º. At this condition, S_T = 1,099 MJ/m² for 2014 solar data, S_T = 1,076 MJ/m² for 2015 data and η_{MO} = 0.7086. This increased S_T by 1.41% and η_{MO} by 1.26% compared to values obtained for α_{s2} = 60º. The variation of α_{s2} also influences the shape of the parabolic reflectors and, consequently, changes the size of the solar collector at the primary section. As α_{s2} decreases, the full width of the collector decreases and the optical efficiency increases, as observed in Figure 6. Hence, the drop of α_{s2} to 50º is positive in terms of absorbed energy and material cost savings. Figure 7 shows the effects of α_{s2} on both reflector cost and overall collector width. Dimensions were obtained from SolidWorks®. Cost calculations were using the price of the reflector sheet provided by the German company ALANOD, which is €50/m².

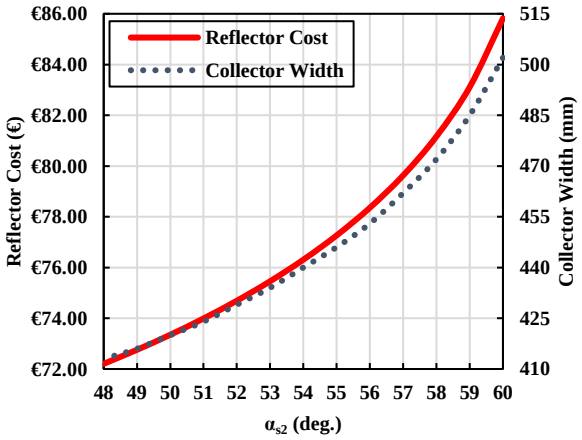

Figure 7: Reflector cost and collector width *versus* angle of the lower parabola axis.

From Figure 7 it is observed that, as α_{s2} decreases, the collector becomes smaller, lighter, and less expensive. This is due to the parabolic shape modifications caused by the rotation of the lower parabola axis. The reflector cost drops from nearly €86 at α_{s2} = 60º to €73.35 at α_{s2} = 50º, reducing the initial design cost by 14.5%.

Regarding the findings of the optical analysis, Table 1 presents the values of the geometric parameters and Figure 8 presents the final collector's shape and dimensions.

Geometry Parameter	**Value**
Aperture Width	330 mm
Absorber Width	145 mm
Concentration Ratio	2.276
Glazing Width	270 mm
Glazing Inclination	66º
Collector Length	1250 mm
Collector Width	424 mm

Table 1: Geometric parameters of the final design.

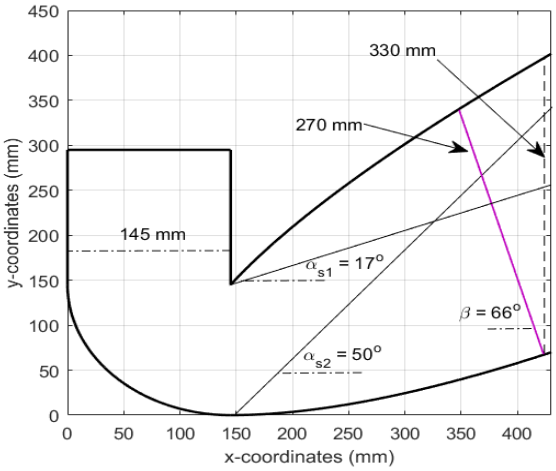

Figure 8: Cross section with dimensions of the solar collector to be fabricated.

Figure 9 shows the optical characterisation of the selected design in terms of η_B, angular acceptance, glazing transmittance, and reflection efficiency as functions of solar altitude angle. The reflection efficiency takes into account only the effect of the average number of reflections.

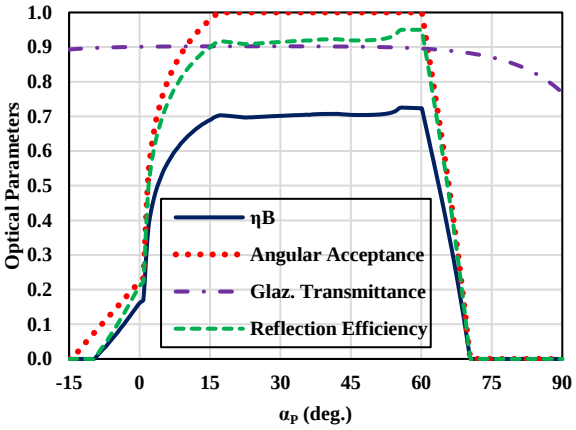

Figure 9: Optical efficiency and angular acceptance *versus* solar altitude angle.

As observed, at the range of 17º – 60º of solar altitude angles, all the incoming rays reach the absorber and η_B lies between 0.6970 and 0.7255. The highest values of η_B are between 55º and 60º of α_p, which is explained by the least number of reflections at the reflectors expressed by the curve of reflection efficiency. The glazing inclination kept the transmittance at 0.9 within the solar altitude range, which minimised the losses through the glass.

Figure 10 presents a graphic of the ray tracing results where it is possible to visualise the path of the incoming rays until they reach the absorber surface.

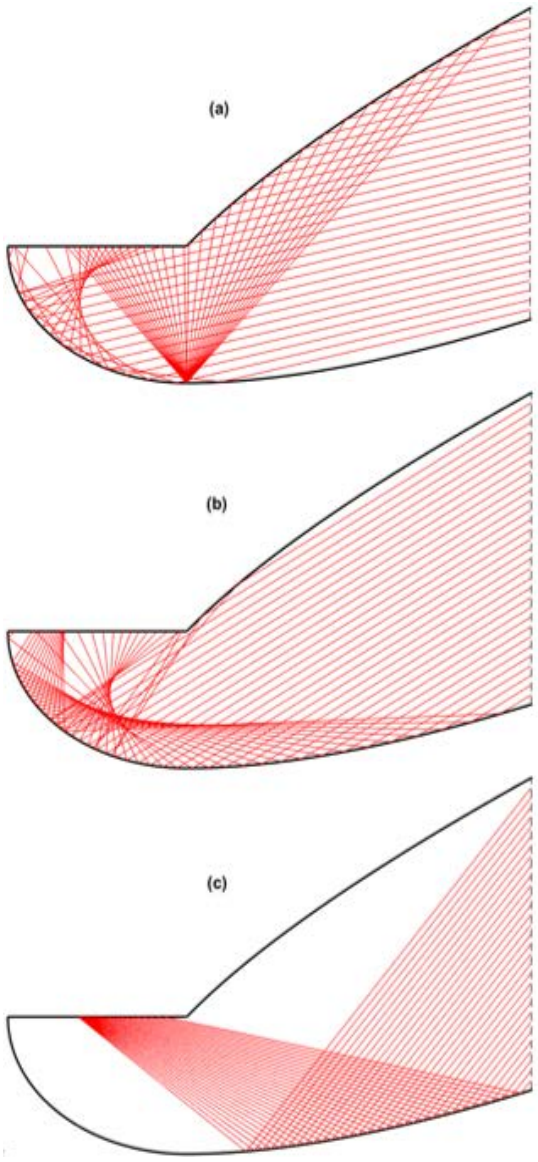

Figure 10: Graphic results of ray tracing for solar altitude angle of (a) 17º, (b) 39º and (c) 60º.

In Figure 10(a) the rays enter the collector at 17º solar altitude angle which is the lower limit of the requirement and α_{s1} = 17º. This means that all the rays that hit the upper parabolic reflector converge to its focal point, at the intersection of the lower parabola and the circular reflector. In Figure 10(c) where α_p is 60º, the upper limit represents the case with the least number of reflections previously mentioned.

To validate the algorithm developed in Matlab®, nine laser tests were performed in a collector prototype. This was fabricated as a cross section of the full-scale collector, made out of the reflector sheet and wooden frames to hold the upper and lower reflector at the selected shape. The visualisation of these tests is presented in Figure 11. Visually comparing these test

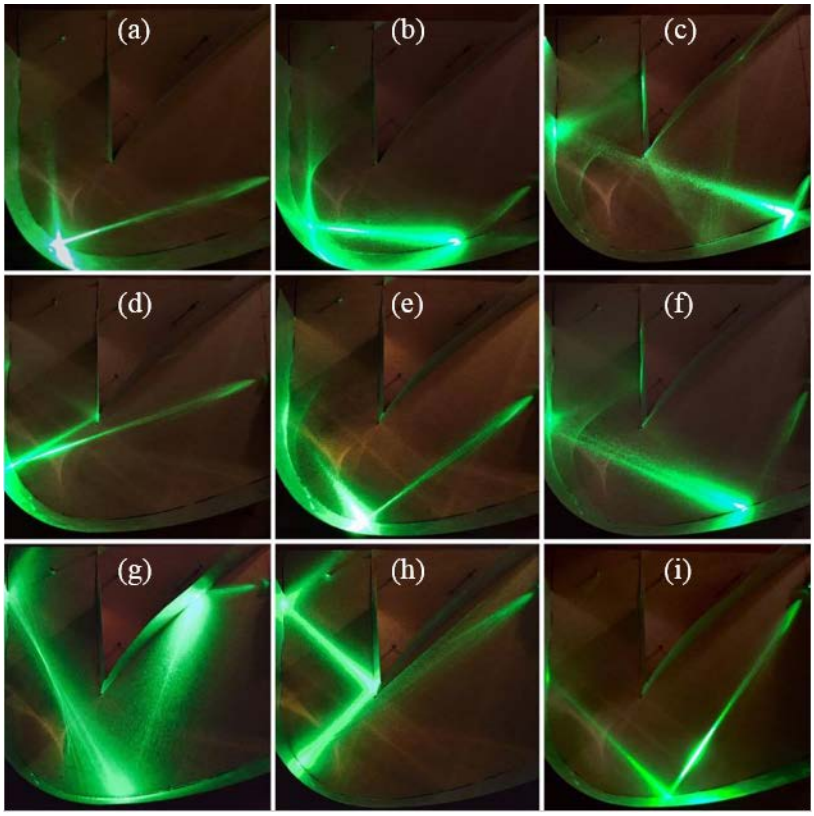

Figure 11: Ray tracing laser test visualisation for three solar altitude angles: 17º in (a), (d) and (g); 39º in (b), (e) and (h); 60º in (c), (f) and (i).

results to the ray tracing results shown in Figure 10, it is possible to conclude that ray tracing is a reliable technique for optical analysis and designing the proposed solar collector.

4 Conclusion

The optimal geometry of the proposed solar air concentrator has been specified. The selection of an air heater IACPC collector with the absorber horizontally facing downwards aims to concentrate solar thermal energy inside the cavity and supress heat losses. With the assistance of ray tracing, an optical analysis has been undertaken to develop the geometry that absorbs the highest amount of thermal energy with the minimum amount of reflective material. For future work, thermal analysis must be conducted along with optical modelling in order to characterise the tertiary section. With the physical prototyping of this solar concentrator, a comparison of the theoretical and actual results will be performed.

5 Nomenclature

C	Concentration Ratio
E	Single ray energy (W)
G_B	Beam solar radiation (W/m^2)
G_D	Diffuse solar radiation (W/m^2)
G_T	Total solar radiation (W/m^2)
n	Average number of reflections
S_T	Total absorbed energy (MJ/m^2)
W_{apt}	Aperture width (mm)
W_{abs}	Absorber width (mm)
α_{abs}	Absorber absorptivity
α_P	Solar altitude angle (º)
α_{s1}	Angle of the upper parabola axis (º)
α_{s2}	Angle of the lower parabola axis (º)
β	Glazing inclination (º)
η_B	Beam optical efficiency
η_{GO}	Global optical efficiency
η_{MO}	Mean optical efficiency
θ	Incidence angle (º)
ρ	Reflector reflectance
τ_g	Glazing transmittance

Subscripts

i	Single Ray
j	Solar altitude angle
k	Second

m	Summer day

6 References

Alta, D., Bilgili, E., Ertekin, C. & Yaldiz, O., 2010. Experimental Investigation of Three Different Solar Air Heaters: Energy and Exergy Analyses. *Applied Energy,* Volume 87, pp. 2953-2973.

Duffie, J. A. & Beckman, W. A., 2013. *Solar Engineering of Thermal Processes.* 4 ed. Hoboken, New Jersey: John Wiley & Sons.

Eames, P. C., Norton, B. & Kothdiwala, A. F., 1996. *The State of the Art in Modelling Line-Axis Concentrating Solar Energy Collectors.* Newtownabbey, WREC.

Goswami, D. Y., 2015. *Principles of Solar Engineering.* 3rd ed. New York: Taylor & Francis Group.

Kothdiwala, A. F., Eames, P. C. & Norton, B., 1996. *Optical Performance of an Asymmetric Inverted Absorber Compound Parabolic Concentrating Solar Collector.* Newtownabbey, WREC.

Kothdiwala, A. F., Eames, P. C. & Norton, B., 1997. Experimental Analysis and Performance of an Asymmetric Inverted Absorber Compund Parabolic Concentrating Solar Collector at Various Absorber Gap Configurations. *Renewable Energy,* Volume 10, pp. 235-238.

Kothdiwala, A. F., Eames, P. C., Norton, B. & Zacharopoulos, A., 1999. Comparison Between Inverted Absorber Asymmetric and Symmetric Tubular-Absorber Compound Parabolic Concentrating Solar Collectors. *Renewable Energy,* Volume 18, pp. 277-281.

Mallick, T. K., Eames, P. C. & Norton, B., 2007. Power Losses in an Asymmetric Compound Parabolic Photovoltaic Concentrator. *Solar Energy Materials and Solar Cells,* Volume 91, pp. 1137-1146.

Rabl, A., 1976. Comparison of Solar Concentrators. *Solar Energy,* 18(2), pp. 93-111.

Shams, N., 2013. *Design of a Transpired Air Heating Solar Collector with an Inverted Perforated Absorber and Asymmetric Compound Parabolic Concentrator*. PhD Thesis. Dublin: Dublin Institute of Technology.

Shams, S. M. N., McKeever, M., McCormack, S. & Norton, B., 2016. Design and Experiment of a New Solar Air Heating Collector. *Energy,* Volume 100, pp. 374-383.

Tyagi, V. V., Panwar, N. L. & Kothari, R., 2012. Review on Solar Air Heating System with and without Thermal Energy Storage System. *Renewable and Sustainable Energy Reviews,* Volume 16, pp. 2289-2303.

Welford, W. T. & Winston, R., 1989. *High Collection Nonimaging Optics.* San Diego: Academic Press.

Wu, Y., 2009. *Thermal Management of Concentrator Photovoltaics.* PhD Thesis. Warwick: University of Warwick.

Zacharopoulos, A., Eames, P. C., McLarnon, D. & Norton, B., 2000. Linear Dielectric Non-Imaging Concentrating Covers for PV Integrated Building Facades. *Solar Energy,* 68(5), pp. 439-452.